RSC Advances

PAPER

View Article Online
View Journal | View Issue

Cite this: *RSC Adv.*, 2024, **14**, 19041

Influence of natural additives on the properties of a milk-based compostable bioplastic†

Raffaella Lettieri, *[ab] Veronica Fazio,[a] Donato Abruzzese, [c] Elisabetta Di Bartolomeo, [a] Cadia D'Ottavi,[a] Andrea Micheletti, [c] Alessandro Tiero, [c] Leonardo Duranti, [a] Valentina Armuzza,[b] Silvia Licoccia [ad] and Emanuela Gatto *[ab]

The ongoing revolution in the plastic sector is the use of renewable and compostable materials obtained from biomass. However, their mechanical strength and thermal stability are generally not sufficient for practical applications. This study investigates the influence of natural additives on the physical-mechanical properties of a new biobased compostable bioplastic, SP-Milk®, produced from milk scraps. To provide this matrix the appropriate mechanical and thermal properties for daily use while leaving its compostability unchanged, the effect of incorporating vegetal fibres and organic particulates into the bulk bioplastic was investigated. Mechanical tests showed that fibres with a length of 2 mm are capable of increasing ductility by up to 97% compared with the original matrix, whereas fibres with a length of 10 mm led to a more effective reinforcement due to the residual resistance effect, increasing the final compressive strain from 20% (original matrix) to 70.9%. The addition of particulate yielded a harder and more resistant material, and the elastic modulus increased by 21%, although with loss of ductility, compared to SP-Milk® alone. The combination of fibres and particles resulted in the preservation of the positive effects of both components, showing a higher elastic modulus (240 ± 20 MPa, compared to 199 ± 12 MPa for the matrix), higher ductility (+50%) and higher strain at failure (+30%), compared with the matrix. Excellent compatibility between the polymeric matrix and both the fibres and the granules was confirmed using scanning electron microscopy. The thermal analysis demonstrated improved thermal stability particularly because of the effect of the combination of granules and fibres. The results validate that natural reinforcement agents are effective and ecologically advantageous.

Received 25th March 2024
Accepted 23rd May 2024

DOI: 10.1039/d4ra02291b

rsc.li/rsc-advances

Introduction

At this historical moment, there is a need that can no longer be postponed, which is developing new innovative materials with revolutionary repercussions on the well-being of society and the planet. Due to the uncontrolled accumulation of fossil-based material waste, environmental safety is becoming a critical issue for the introduction of new materials. Globally, annual plastic production has increased from 234 million tonnes (Mt) in 2000 to 460 Mt in 2019. Plastic waste increased by 126% (from 156 Mt in 2000 to 353 Mt in 2019). Of these, only 9% were recycled, 19% were incinerated, and about half ended up in sanitary landfills. The remaining part (22%) was disposed of in uncontrolled landfills, burnt or dispersed in the environment.[1] The main market for plastics is for short-term applications (single-use items and packaging), for which most of the materials used are derived from fossil and non-biodegradable polymers. According to data reported by the Minderoo Foundation in the Second Plastic Waste Makers Index,[2] the world generated 139 Mt of single-use plastic waste in 2021, which was 6 Mt more than that in 2019 when the first index was released. Bioplastics are plastics that are biobased, biodegradable, or both. One of the major advantages of biobased plastics, compared to conventional fossil-based polymers, is the use of biomass as raw materials, which regenerates, unlike fossil resources.[3] Based on what has been reported by the European Bioplastics, applications for bioplastics are growing, from packaging to electronics, automotive, and textiles. Packaging is the biggest market segment for bioplastics, reaching 43% of the entire market of bioplastics in 2023. The design of a new material must consider its management during all phases of its life, paying particular

[a]University of Rome Tor Vergata Department of Chemical Science and Technologies, Via Della Ricerca Scientifica, 00133 Rome, Italy. E-mail: raffaella.lettieri@uniroma2.it; emanuela.gatto@uniroma2.it

[b]Splastica Srl, Via Del Lavoro 13, 00045 Genzano di Roma, Rome, Italy

[c]University of Rome Tor Vergata Department of Civil and Computer Science Engineering, Via Del Politecnico, 1, 00133 Rome, Italy

[d]NAST Centre for Nanoscience, Nanotechnology and Instrumentation, University of Rome Tor Vergata, Physics Department, Via Della Ricerca Scientifica, 00133 Rome, Italy

† Electronic supplementary information (ESI) available. See DOI: https://doi.org/10.1039/d4ra02291b

attention to its disposal after use. Therefore, great efforts are expected from the scientific community to identify safer alternative chemical ingredients to obtain materials that can replace fossil-based ones. In the last decade, important scientific advances have been achieved on different kinds of biomass-based materials, such as bioplastics and biobased films and inks, with the aim of replacing petroleum-derived products with biomass-based ones.[4] Nevertheless, so far, biomass-derived materials exhibit poor mechanical properties that make them not competitive compared to conventional materials. Common methods (*i.e.* cross-linking, heat curing, and radiation) can be used to improve their performance, but these methods can present drawbacks because the reactions can be difficult to control and create damage to the polymer chain.[5] Among the most common reinforcement agents, synthetic fibres, such as glass, aramid, and carbon fibres, can improve the performance and lightness of a material,[6] but they can have dangerous effects on health and a high environmental impact.[7] Due to high raw material costs and environmental issues, great interest has been placed in the development of green composite materials, where a bulk material derived from renewable resources is combined with natural reinforcement and/or filler agents, thus achieving diverse technical and economic improvements.[8] In many cases, natural-reinforced materials are lightweight, more flexible, totally or partially renewable, processable, and less irritating to the skin than traditional composites. However, some disadvantages can occur and must be implemented, such as moisture absorption, lower durability, and inhomogeneity, due to irregular geometries of the additives.[9] Among the numerous natural additives, natural fibres can improve the properties of a material with technical, economic, and ecological advantages. Due to their excellent mechanical and physicochemical properties, natural fibres have been the subject of numerous studies[10–12] and have recently gained prominence when manufacturing composites as alternatives to synthetic fibres, sparking the interest of many industries that have moved to use environmentally friendly products to reduce dependence on fossil fuels.[13] Venkateshwaran *et al.* found that natural fibres can advantageously reduce the weight of epoxy composites by increasing their mechanical properties and decreasing moisture absorption.[14] Bisaria *et al.* investigated jute fibre-reinforced composites by analysing the effect of fibre length on tensile, flexural, and impact properties.[15] A further step toward sustainability is achieved when all the materials are chosen to produce a composite derived from biomass, providing a fully biobased composite.[16] The addition of selected natural components to a biodegradable matrix allows for maintaining biodegradability while reinforcing a poorly mechanically performant biomaterial.[17] In addition to the use of natural fibres, the addition of fillers of natural origin has also been reported in the literature. Among these, walnut shells have shown interesting properties. Monika *et al.* found that the addition of walnut shells to polypropylene-based composites improved the thermal stability of the material.[18] Ahlawat *et al.* demonstrated that by increasing the walnut shell weight in a polyester matrix, the tensile modulus increased, but the flexural modulus and tensile strength decreased.[19] Moreover, a significant environmental and economic impact results from the use of waste as raw material for obtaining both the matrix and additives. Organic waste is an abundant, inexpensive source of raw materials and represents a powerful matrix for the development of biomaterials due to the abundance of biomolecules in the scrap. According to FAO, 14% of food is globally lost from harvest up to, but not including, retail.[20] Agri-food waste, generally incinerated or discarded, causes air pollution and reduces soil biological activity[21] and is accompanied by environmental impacts, such as soil erosion, deforestation, air and water pollution, and greenhouse gas emissions, that occur in the processes of food production, storage, transportation, and waste management. Further use of these residues is, however, possible; they represent a potential source of animal feed and can also be converted to bioenergy and other useful and valuable products. Thus, this type of waste can be considered a by-product that becomes an important resource and re-enters the production chain in accordance with the principles of a circular economy. The use of agricultural waste combined with polymer matrices is an interesting research topic due to the possibility of modulating the strength, stiffness, and density of composites owing to the action of the components present in these types of residues,[22,23] which are mostly proteins and polysaccharides. Protein-based materials, with respect to polysaccharide-based ones, are more useful for applications that require gas barrier properties, and the mechanical features are more suitable for many purposes.[5] This is due to the intermolecular binding potential of the proteins, which makes it possible to confer many different functional properties to the final material.[24–26] Bioplastics based on these components are affected by several limiting disadvantages (stiffness and brittleness, discontinuity when formulated with no additives and plasticizers)[27,28] and the need for solutions, often environmentally impacting, for thermoplastic processing.[29] The bulk polymeric material object of the present work is called SP-Milk®, an innovative biomaterial produced from organic waste, in particular from milk scraps, 100% based on natural polymers, biodegradable and home compostable according to the European technical standard UNI-EN 13432. It has been produced by Splastica®srl through a new eco-friendly procedure to extract natural biopolymers from biomass and convert them into a biomaterial. SP-Milk® exploits the intrinsic thermoplastic properties of proteins for the fabrication of items similar to plastic but without the exploitation of fossil fuels. For these reasons, SP-Milk® represents a good sustainable bulk material for the manufacturing of several objects, but its mechanical properties are not as performing as those of fossil-based plastic. To give this matrix the appropriate properties for daily use but at the same time make the material safe and with a low environmental impact, the effect of adding natural substances was investigated. In particular, fibres derived from the hemp plant (0.1–1.0 wt%) and organic filler particulate made of powdered walnut shells (10–40 wt%) were incorporated into the protein-based bulk bioplastic, and the obtained composites were investigated. The choice of additives and their quantity was made to ensure that the objects could maintain their hygroscopicity, ensuring good mechanical properties and biodegradation if accidently

discarded in the environment. Moreover, the nature of all the additives used to improve the bulk material, which is defined as compostable by the producer, makes us confident that such an addition will not make the material less environmentally friendly but will improve its performance to make it concretely useful for the intended applications. The sustainability of the materials concerns the impact on climate change, the land and water use and the economic analysis, as the raw materials used are all by-products of the agri-food chain. This represents a great advantage because something that should be considered a waste becomes a new material.

Experimental

Materials

All the samples have as a matrix the protein-based material called SP-Milk®, whose protein content is almost half of the total weight. Nine samples (refer to Table 1) were prepared, with one sample consisting of the matrix material and the remaining eight containing the matrix material along with biobased additives of different nature: (a) fibrous component consisting of hemp fibres of two lengths: short fibres of 2 mm (SF) added to the matrix at different weight percentages (0.1, 0.5, and 1.0 wt%); long fibres of 10 mm (LF) added at 1.0 wt%; (b) an inert filler made of powdered walnut shells in the form of semi-hard granules with dimensions in the range of 2–100 μm, named IG (inert granules), at a weight percentage of 10, 20, and 40 wt%; (c) a mixture of the components (a) and (b), named LF/IGmix, formed by adding 20 wt% of inert filler and 1 wt% of long fibres. The fibres selected to reinforce the matrix are skin fibres collected from the skin or bast surrounding the stem of their plant. Hemp fibers are characterized by a higher tensile strength with respect to other natural fibres.[30] The LF/IGmix sample was useful for assessing the effect of the co-presence of filler and fibres.

Specimen fabrication for mechanical tests

The specimens for the mechanical tests were prepared by compression moulding, imparting a pressure of about 15 kPa on the material in its soft state, which was shaped inside specific-made moulds to obtain specimens of suitable geometry for mechanical testing according to reference standards. We obtained the moulds using ABS on a 3D printer. The SP-Milk® composites were synthesized by mixing the natural additive (hemp fibres and/or granulate from nut shells in the proportion reported in Table 1) with the polymeric matrix in its soft state obtained by heating the granules with water, subsequently moulding to obtain the specimens and air drying at room temperature. The samples were made of suitable geometry according to the standards applicable to studying the properties of reinforced composite materials: ASTM D695-15 (2015)/ISO604 (2002) for compressive tests and ASTM D790 (2017)/ISO 178 (2019) for flexural tests. Rods with rectangular cross sections of sizes 12.7 × 12.7 × 25.4 mm and 127 × 16 × 13 mm were prepared for the compressive and flexural tests, respectively. To ensure reliability, we performed each measurement in triplicate.

Table 1 List of abbreviations and description of the type and amount of additives in the composite materials

Sample	Additive description	wt% additive
SP-Milk	No additives	—
SF 0.1%	Short hemp fibres	0.1
SF 0.5%	Short hemp fibres	0.5
SF 1.0%	Short hemp fibres	1.0
LF	Long hemp fibres	1.0
IG 10%	Inert granules of walnut shell	10
IG 20%	Inert granules of walnut shell	20
IG 40%	Inert granules of walnut shell	40
LF/IGmix	Long hemp fibres + inert granules	1/20

Mechanical tests

The compression tests were made using an Instron 4482 test machine configured for compressive tests with a 10.0 ± 0.1 kN load cell, applying a load at a constant displacement rate of 0.500 ± 0.005 mm min^{-1}, at room temperature. The tests were carried out up to the minimum height limit of the specimen, which was established at 1 cm. The (nominal) stress (σ) was calculated by dividing the force acting on the specimen by the transverse original area of the specimen. The force and stress acting on the specimen were plotted as a function of displacement and as a function of strain (ε), respectively. The use of a trilateral curve was preferred to simplify the data comparison and interpretation. The approximation consists of replacing the σ–ε curve with a polygonal curve composed of three line segments with angular coefficients E_e (elastic modulus), E' (hardening modulus) and E'' (coefficient of rupture). The vertices of the polygonal different from the origin (O) define the characteristics of the Yield Stress Point (YSP), Maximum Stress Point (MSP) and Ultimate Stress Point (USP). The mechanical meaning of these points is as follows: YSP represents the limit between the elastic and plastic zones, MSP is the maximum hardening point, and USP is the breaking point (ESI Material, S1†). The modulus of elasticity or Young's modulus (E_e) and the Deformation Energy (DE) were computed: first, from the slope of the tangent to the σ–ε curve in the region of linearity and second, from the area under the σ–ε curve. The curves reported are obtained by averaging the results of the three tests. Flexibility properties were tested on the same machine used for compressive tests and configured for the three-point bending tests in displacement control. The sample was placed equidistantly from the two support points ($L = 120$ mm) in the fixed crossbar; the mobile crossbar, which is connected to the load cell, applies the load on the central point of the sample, moving at a crosshead speed of 0.500 ± 0.005 mm min^{-1}. As required by ISO 178, the test stops when the sample is broken. The hardening zone is not noticeable in the flexural load (F) – displacement (δ) curve or is very small: the part preceding the maximum strain point is very short or absent, while the rupture is faster and steeper than the compression test. In this case, the yield stress point (YSP) is defined as the intersection of the straight line of slope E for the origin and the horizontal line for the maximum stress point. Therefore, a bilateral curve with vertices O, YSP and USP was chosen to approximate the average

data. The bending test apparatus, the specimen geometry and the bilateral approximation of the load–displacement curve are shown in ESI Materials, S2.†

Thermal analysis

Differential Scanning Calorimetry (DSC) measurements were performed in N_2 at 50 mL min^{-1} using a Star System Mettler Toledo DSC1 and DSC 214 Polyma with NETZSCH calorimeter. The samples were kept for 1 h at 50 °C. To ensure good contact between the sample and the bottom of the pan and minimize the temperature gradient in the samples, they were pulverized with a laboratory mortar so that the very fine particles could create a homogeneous layer on the base of the pan. The powder was then pressed to obtain a thin compact disk-shaped sample. In the first run, the samples were heated from 30 °C to 100 °C (5 °C min^{-1}); the temperature was kept at 100 °C for 5 min to allow water evaporation. The samples were cooled at 30 °C (10 °C min^{-1}) and heated again up to 200 °C (5 °C min^{-1}). A heating rate of 5 °C min^{-1} was used to increase resolution, minimizing the temperature gradient within the sample. Simultaneous Thermogravimetric Analysis and Differential Scanning Calorimetry (TG-DSC) in air were performed using a Mettler Toledo TG-DSC 1, Star System. The samples were kept for 1 h at 50 °C and then reduced in powder. Samples were first heated up to 100 °C for 5 min (5 °C min^{-1}) for excess water evaporation. Then, the samples were cooled and heated again up to 600 °C (10 °C min^{-1}).

Morphological analysis

After mechanical stress, the morphology of the sample fractured surfaces was investigated using a field-emission gun scanning electron microscope (FEG-SEM, Cambridge Leo Supra 35, Carl Zeiss) after sputter-coating with gold under an argon atmosphere (25 mA, 120 s).

Moisture analysis

Moisture analysis was performed using OPTIKA Balance Italy by heating the samples from room temperature to 100 °C, with a ramp of ~50 °C min^{-1}. The temperature was then kept stable until the percentage humidity loss decreased below 0.1% for 20 s.

Results and discussion

Compressive tests

A comprehensive evaluation of the mechanical properties was investigated by compression tests, providing information about material integrity under stress conditions. From the uniaxial compression of the samples, the compression stress (σ) *versus* strain (ε) curve was calculated and reported in Fig. 1 as a trilateral approximation.

Table 2 presents a report of average elastic modulus E_e, the Deformation Energy (DE) value, the hardening modulus E', the coefficient of rupture E'', the characteristic points YSP and MSP, and the ratio between ultimate displacement (δ_U) and yield (elastic) point displacement (δ_Y), indicating the ductility of the sample. The bulk material SP-Milk® (Fig. 1A) showed poor compression strength. An elastic behaviour of up to 3% strain and crushing at 23% strain were observed. By considering the ratio between ultimate displacement and yield (elastic) point displacement (δ_U/δ_Y), moderate ductility under low stress can be observed. To improve its performance, the cited natural additives were added to SP-Milk®. Compression tests of specimens with fibres (Fig. 1B) gave the expected results, *i.e.* the decrease in both Young's modulus and YSP, and the increase in ductility. In particular, the addition of short fibres resulted in a decrease in both MSP and YSP, an increase in the maximum strain together with the elastic modulus value with respect to parent SP-Milk®. These data indicate that the fibrous composite exhibits greater flexibility compared to the matrix alone, even if the maximum load resistance is lower. The hardening coefficient, the branch in which the effect of the fibres on the matrix is visible, is higher in modulus than the crushing coefficient, indicating a plastic behaviour. A slight dependence on the amount of fibrous filler was observed, moving from 1.0 to 0.5 wt%. The deformation energy increases more than those of the matrix, while both E' and E'' decrease. The ductility of SF 1.0% is higher with respect to the matrix and the lower percentages of fibres. The greatest improvement in ductility is achieved with fibres at 1 wt%. SF 1.0% can be defined as a tenacious-elastic material. The observed effects are attributable to the resistance to internal flows, which are attenuated by the fibrous component. The random distribution of the fibres leads to a slow deformation with the samples showing poor resistance to the load. With the addition of short fibers, the greatest improvement in ductility is achieved using a higher amount of this additive. Therefore, we moved to longer fibers by maintaining the same weight percentage to verify whether an improvement could be observed only as a consequence of the fiber length. The use of longer fibres (sample LF) leads to a more effective reinforcement of the matrix. A final compressive strain of 70.9% is achieved, and an improvement in ductility is observed. The fibres dampen the flows, leading to a second stage of hardening (ESI Material, S3†). This behaviour corresponds to a neutral rupture in which the constituent confers residual resistances, yielding more than one MSP and resulting in a high toughness: the total area under the stress–strain diagram is larger. This indicates that the composite material under analysis can undergo more permanent deformation than the matrix alone before fracture occurs. The transfer of load gives the effectiveness of the reinforcement during the formation and propagation of cracks from the matrix to the fibres for the so-called residual resistance effect. After the formation of the first crack, the composite exhibits a ductile behaviour, that is, it can tolerate additional loads owing to the action of the fibres. The addition of granules imparted interesting characteristics to the material. For the IG samples (Fig. 1C), no significant differences in E_e were detected. The hardening branch is shorter with respect to SP-Milk® corresponding to lower strain % values. In particular, in comparison with SP-Milk®, IG 10% showed a slight decrease in E_e and YSP, resulting in lower resistance. E'' is comparable to SP-Milk®, but the final strain reaches a higher value, showing improved ductility (Fig. 1C, blue line), as can also be assumed considering

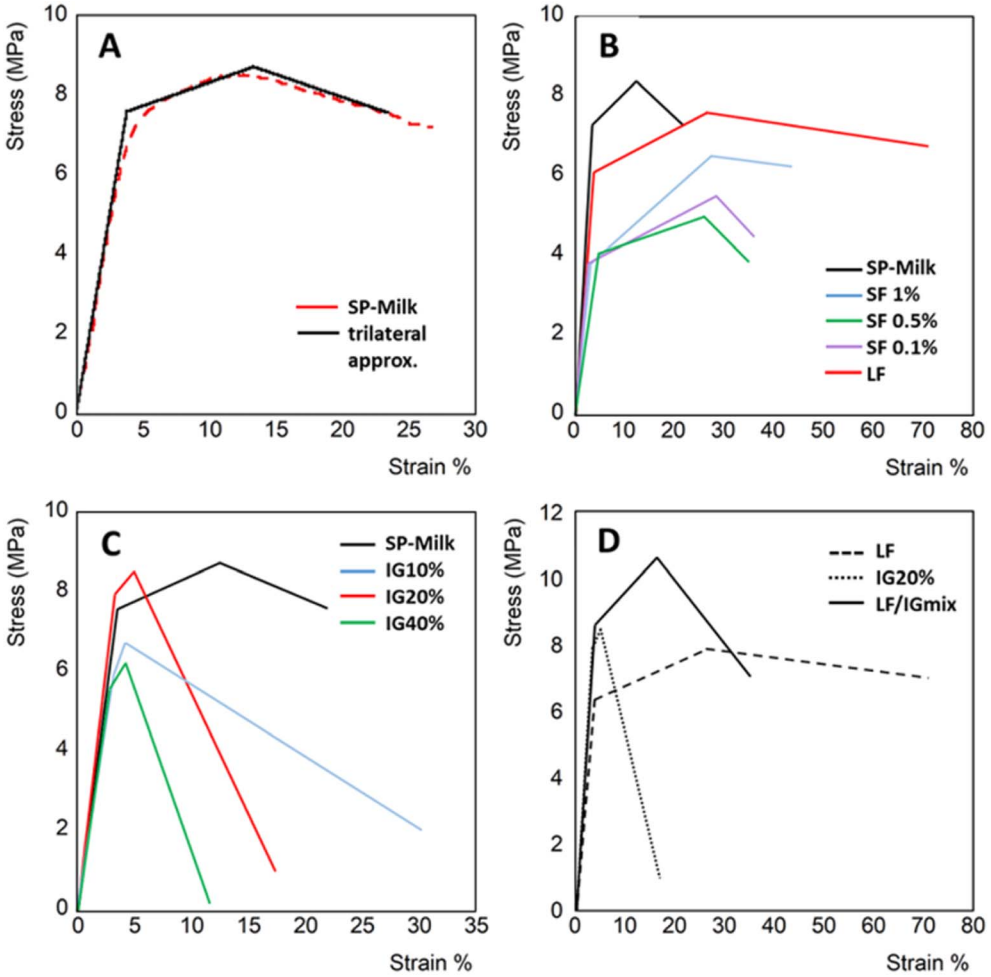

Fig. 1 Trilateral approximated compression stress *vs.* strain curves obtained for SP-Milk, overlapped to the original graph, in red (A); comparison between SP-Milk, in black, and fibrous composites (B); SP-Milk compared to samples with inert granules (C); comparison between LF, IG 20% and LF/IGmix (D).

Table 2 Characteristic points and angular coefficients obtained from compression testing of SP-Milk® matrix and composite materials

Sample	E_e (MPa)	DE (J mm^{-3})	YSP (MPa)	E' (MPa)	MSP (MPa)	E'' (MPa)	δ_U/δ_Y
SP-Milk	199 ± 12	29 ± 1	8 ± 1	13 ± 4	9 ± 1	−12 ± 4	6.5
SF 0.1%	120 ± 20	29.6 ± 0.2	4.0 ± 0.2	7.6 ± 0.4	5.7 ± 0.2	−1.2 ± 1	10.7
SF 0.5%	80 ± 20	33.5 ± 0.2	4.3 ± 0.2	6 ± 1	5.2 ± 0.2	−1.2 ± 1	7.1
SF 1.0%	110 ± 10	25.1 ± 0.1	4.0 ± 0.1	13.0 ± 0.2	6.8 ± 0.1	−1.6 ± 0.1	12.8
LF	150 ± 10	27.80 ± 0.05	6.36 ± 0.05	6.9 ± 0.1	7.90 ± 0.05	−6.1 ± 0.3	17.1
IG 10%	180 ± 10	16.0 ± 0.2	6.0 ± 0.2	73.2 ± 0.4	6.7 ± 0.2	−18 ± 1	9.2
IG 20%	240 ± 10	27.3 ± 0.3	7.9 ± 0.3	34 ± 2	8.5 ± 0.3	−60 ± 10	5.2
IG 40%	220 ± 10	17.5 ± 0.2	5.3 ± 0.2	44 ± 1	6.1 ± 0.2	−80 ± 20	4.8
LF/IGmix	240 ± 20	36 ± 1	9 ± 1	16 ± 3	11 ± 1	−20 ± 10	9.7

the δ_U/δ_Y value. The addition of 20% of an inert component leads to a harder and more resistant material, considering the increase in E_e and YSP with respect to IG 10%, even if ductility is lost (Fig. 1C red line). IG 40% is the less-performing sample, showing poor deformation energy and low ductility. The material maintains its strength over a restricted range of plastic deformation. To improve the matrix, taking advantage on the one hand of the ductility given by the reinforcement of long fibres and on the other hand of the higher load resistance imparted by 20% of granules, a composite material, named LF/IGmix, was manufactured by adding both components to the matrix, selecting the most efficient weight percentage. As expected, LF/IGmix shows both the hard behaviour of the granules and the ductility of the fibres. In fact, as can be observed in Fig. 1D and considering the data reported in Table 2, it showed higher resistance to elastic deformation, higher YSP and MSP,

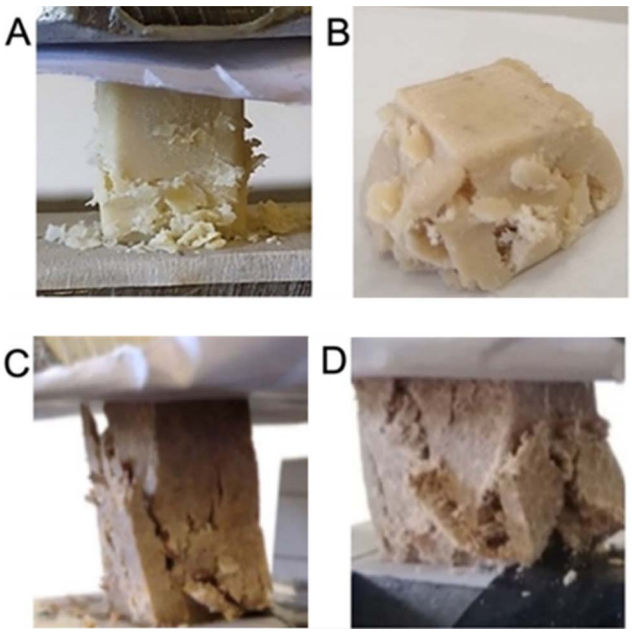

Fig. 2 Appearance of the samples after the compression test. SP-Milk® (A), LF (B), IG 20% (C), and LF/IGmix (D).

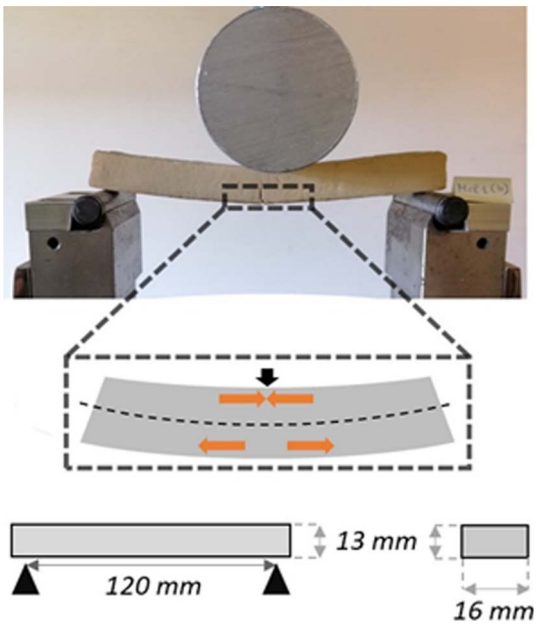

Fig. 3 Representation of forces acting on the area above the neutral axis during the flexural tests.

both considering the maximum stress and strain %, and it reaches a higher strain % at failure. Observing the appearance of the samples SP-Milk® (A), LF (B), IG 20% (C), and LF/IGmix (D) after the compression test, it is possible to observe the effects on the material under stress during the crushing phase (Fig. 2). SP-Milk® (Fig. 2A) shows clearly visible fractures. The presence of fibres causes a very intense deformation with fractures, which, however, tends to leave the specimen more unified (Fig. 2B). This result agrees with what is deduced from the overall data: the fibres act as reinforcements and provide residual resistance to the structure. This is also observed in LF/IGmix (Fig. 2D) even though the presence of granules makes this sample more brittle (well visible in IG 20%, Fig. 2C).

Flexural tests

Flexural tests were performed to better analyze the behavior of materials under mechanical solicitation. During bending stress, the area of the specimen above the neutral axis is subjected to compression with densification of the constituents of the material, while the area below the neutral axis is subjected to a tensile force, with distension of the material (Fig. 3).

From the results of the bending test, another elastic modulus can be calculated, which can be compared with that calculated from the compressive test. The elastic modulus, reported in Table 3 as E, was extracted considering the part of the curve where the material shows linear elastic behavior, the shape of the specimen, and the geometry of the loading procedure. In particular, considering the linear proportional zone of the loading curve, the displacement from the neutral plane (δ) is related to the elastic modulus (E) by the following equation: $\delta = FL^3/(48EI)$, where L is the distance between the supports and I is the moment of inertia (which for a solid rectangular section is equal to $bh^3/12$). Fig. 4 shows the flexural behaviour of the specimens, with the approximated curves of load and middle displacement of the beam.

Table 3 Results obtained from flexural tests on matrix and composites

Sample	F_{max} (kN)	δ_{max} (mm)	E (MPa)
SP-Milk	0.061 ± 0.001	2.782 ± 0.002	433 ± 23
SF 0.1%	0.054 ± 0.002	2.8 ± 0.1	409 ± 8
SF 0.5%	0.041 ± 0.001	3.6 ± 0.1	293 ± 23
SF 1.0%	0.049 ± 0.001	5.6 ± 0.1	198 ± 21
LF	0.058 ± 0.001	5.26 ± 0.07	340 ± 15
IG 10%	0.044 ± 0.002	2.6 ± 0.1	296 ± 43
IG 20%	0.055 ± 0.001	2.2 ± 0.1	281 ± 54
IG 40%	0.064 ± 0.002	1.9 ± 0.1	491 ± 63
LF/IGmix	0.118 ± 0.002	3.11 ± 0.06	622 ± 13

For SP-Milk®, the failure is of a rigid type with almost absent resistance, demonstrating the stiffness and fragility of the matrix alone. The matrix shows high resistance to bending load, which is poorly flexible and brittle. The addition of fibres gave encouraging results in the case of short fibres in a higher percentage (SF 1.0%) and the case of long fibres (LF). Observing the data reported in Table 3, by increasing the percentage of short fibres, an increase in the maximum displacement and a decreasing trend of the elastic modulus occur. Moreover, as the percentage of short fibres increases, the failure becomes increasingly ductile, as can be deduced by comparing the slope of the curve at the breaking point. The use of longer fibres leads to effective reinforcement, as already observed in compression tests. While tolerating a slightly lower load with respect to the matrix, the presence of long fibres makes the material more flexible. Among the IG specimens, IG 40% is the only one showing a flexural strength comparable to the matrix, but the

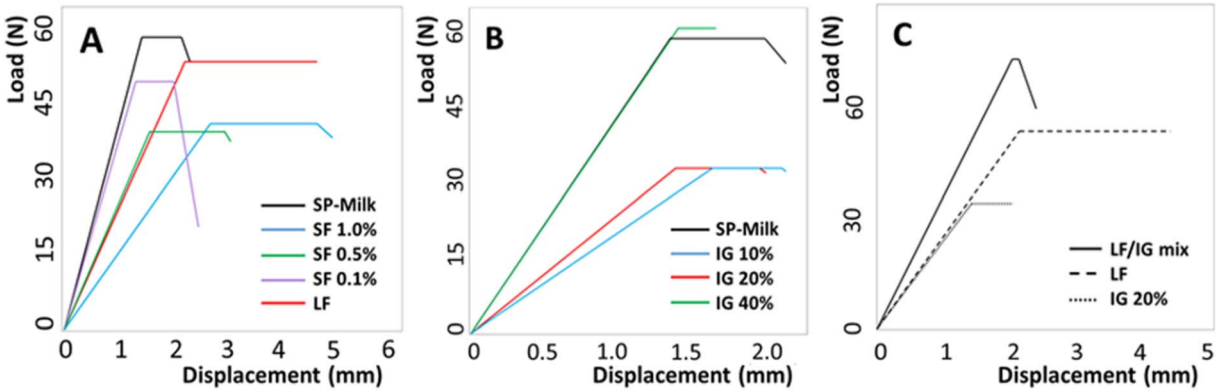

Fig. 4 Flexural behaviour-approximated curves: SP-Milk® compared to fibrous composites (A); SP-Milk® compared to samples with inert granules (B), comparison between LF, IG 20% and LF/IGmix (C).

deformability is lower. Samples IG 10% and IG 20% reached lower loads with respect to SP-Milk® and similar deformations. The best compromise between bending displacement and strength is achieved for IG 20% even if this additive alone does not lead to an improvement in the matrix. The composite LF/IGmix shows successful reinforcement as the maximum load reached is higher than that of the matrix.

From the data obtained and considering the Ashby plot showing strength *vs.* Young's modulus of common polymers, it is possible to state that the SP-Milk-based composites can reach Young's modulus and yield strength values, which fall within the range reported for common polymers. In particular, it is reported that Young's modulus of polymers covers the range of 0.1–10 GPa and the yield strength can vary from about 4 to 100 MPa. A significant comparison can be performed with thermoplastic polymeric materials, such as low-density and high-density polyethylene, for which their compressive strengths at room temperature are reported to be 10.7 ± 0.7 MPa and 23.0 ± 0.8 MPa,[31] respectively. Among thermoplastic materials, thermoplastic starch has a relevant position in the field of environmentally friendly materials for replacing fossil-based plastics although it has poor mechanical properties, such as low tensile strength and severe deformation, which limits its areas of application. Blending with other polymers is an effective way to overcome these drawbacks, but this is often done using fossil-based polymers. Furthermore, starch-based plastics show variable properties due to the diversity of the starch molecular structure.[32] The major advantage of SP-Milk-based bioplastic is that it is fully biobased and not blended with polymers of fossil origin.

Differential scanning calorimetry measurements

Differential scanning calorimetry measurements allowed for determining the glass transition temperature (T_g) of the samples, indicating the amorphous nature of the matrix. DSC curves of the most relevant samples (reported in Fig. 5) showed a second-order transition, and the inflection point corresponds to the T_g. The following values were obtained: SP-Milk® 148 °C; LF 137 °C; IG 20% 115 °C; LF/IGmix 123 °C. These values are compatible with the values reported in the literature for anhydrous casein, which is 144 °C.[33,34] The addition of different natural components decreased the T_g value of the SP-Milk® matrix. This modification might be attributed to the tendency of the additives that come from plant matrices to be susceptible to water. In fact, both walnut shells and hemp fibers are rich in cellulose, hemicellulose, lignin and pectin, containing many hydroxyl groups. The presence of these functional groups leads to an increase in the hydrophilicity of the final material. Such behaviour increases chain mobility and consequently decreases the matrix glass transition, in which water is one of the most important plasticizers. The differences observed in the T_g values may also be related to heat dissipation differences as a result of the presence of the fillers. This achievement is noteworthy because the industrial processing of polymeric materials by different molding techniques requires exceeding this temperature value to make the material malleable. Lowering the T_g makes the material machinable with a significant reduction in energy requirements and costs.

Thermogravimetric analysis

Simultaneous Thermogravimetric Analysis and Differential Scanning Calorimetry (TG-DSC) measurements were performed in air to study the thermal stability of the samples. Fig. 6a shows the TG and DSC curves, together with the DTG profiles (dotted lines), for the SP-Milk® matrix. As expected, no weight loss due to water evaporation could be observed, as a preheating run was performed to eliminate the contribution of water. The complete TG-DSC profiles for LF, IG 20% and LF/IGmix are reported in ESI Materials, S4.† SP-Milk® is stable up to around 160 °C. The obtained curves highlight the presence of three main weight loss regions in the following ranges: 180–240 °C (I), 240–330 °C (II) and 330–390 °C (III) (Table 4).

Region I is associated with the weight losses due to the evaporation of the plasticizer and to the first stage of casein chemical degradation.[35–37] Regions II and III show two partially superimposed peaks, which indicate two reactions that rapidly occur in the 240–400 °C range. The sharp contribution in Region II can be attributed to the initial decomposition of larger molecular weight components, while the broad one in Region III results from the second stage of decomposition of casein. For

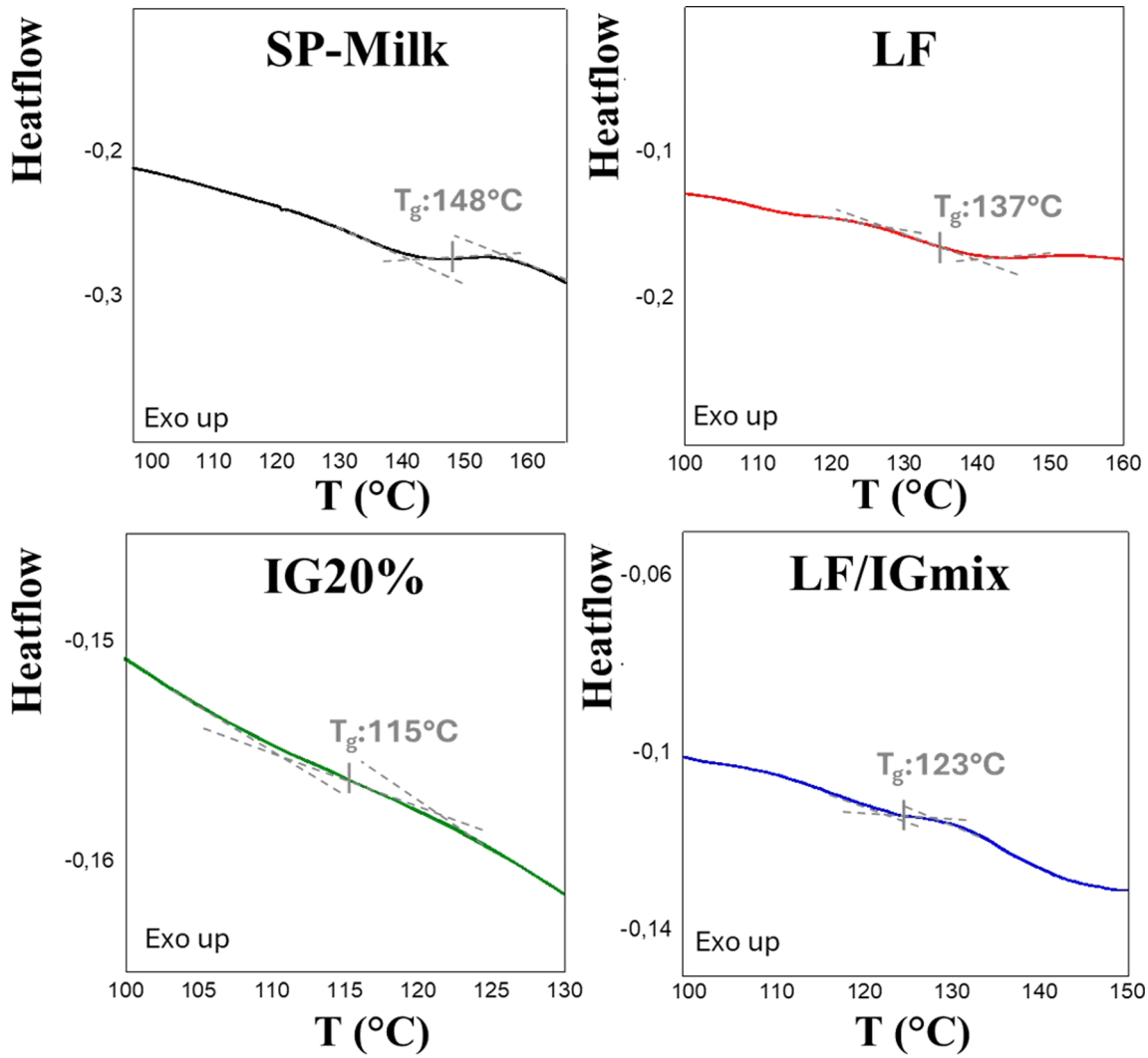

Fig. 5 Differential scanning calorimetry thermograms of the samples during the second heating run. The glass transition temperature values were determined using a midpoint calculation.

$T > 400$ °C, the combustion of casein mainly occurs. For all the samples, a residue of about 20% was observed because the final temperature reached in the experiment was not high enough to cause the complete sample combustion. Casein is not expected to show a residue in the air if heated up to at least 780 °C.[36] Although T_1 and T_3 are negligibly affected by the presence of the different fillers, T_2 values confirmed that the LF/IGmix composite sample showed a positive interaction between the filler and matrix. A zoom in the DTG profile around T_2 is reported in Fig. 6b for all the tested samples. The LF/IGmix composite is the only one featuring a $\Delta T_2 = 5$ °C with respect to the SP-Milk® matrix, suggesting a positive effect of the combination of the two components not only on the mechanical properties but also on the thermal stability. The thermal stability of the presented biomaterials is extremely important because one of the most limiting features of many bioplastic materials is their deterioration when in contact with heat.

Moisture content

Moisture is a fundamental parameter that must be considered to understand a material behaviour because water acts as a plasticizer affecting the T_g and therefore processability.[38,39] The moisture content of SP-Milk® is $3.4 \pm 0.3\%$. The values measured for LF, IG 20%, and LF/IGmix are $4.9 \pm 0.4\%$, 4.7 ± 0.2, and 4.5 ± 0.4, respectively (ESI Materials, S5†). Moisture content analysis revealed that changes made to the SP-Milk® matrix increased its water content, in agreement with what was assumed based on the DSC results. The presence of a higher content of water reflects a decrease in the T_g. The increase in this parameter in all the composites studied is due to the hydrophilic characteristics of the additives, as already discussed in the differential scanning calorimetry measurement paragraph.

SEM analysis

SEM micrographs of the fractured surfaces after the bending tests are presented in Fig. 7. SP-Milk®, SF, LF, IG 20% and LF/

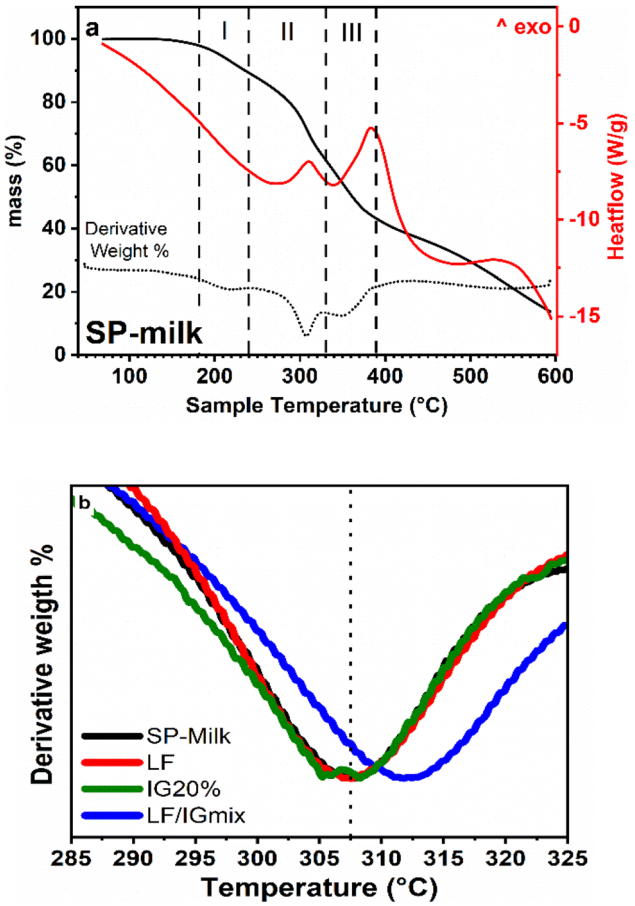

Fig. 6 (a) Thermal analyses of the SP-Milk matrix: TG (solid, black), DTG (dotted, black) and DSC (solid, red) *vs.* temperature. Complete profiles for LF, IG 20% and LF/IGmix samples are reported in ESI Materials, S4;† (b) zoomed section of the DTG profiles, highlighting the T_2 area for all the tested samples.

Table 4 Peak temperatures derived from the DTG profiles

Sample	T_1 (°C)	T_2 (°C)	T_3 (°C)
SP-Milk®	217	307	328–380
LF	225	307	330–402
IG 20%	226	307	324–375
LF/IGmix	229	312	332–397

IGmix samples are shown. After the three-point bending test configuration, the stress experienced by the rupture zone below the neutral axis can be considered a tensile stress. In this area, the formation of fibrils and microcavities causing the formation of cracks, due to the tension following the stretching of fibrillar bridges, should be observed. On the fractured SP-Milk® sample, the globular nature of the polymer surface is observable (Fig. 7a and b). The morphology is homogeneous, confirming the stiff and brittle nature observed under bending stress, which agrees with the mechanical data. At higher magnification (Fig. 7b), microcavities due to the sudden detachment of the two sample ends are observable. However, the SF fractured sample shows the short fibres pulled out of the surface (Fig. 7c). The polymeric matrix is deformed following the direction of the fibres. Fig. 7d presents the zoomed detail of a single short fibre. It is possible to observe how the matrix polymer film covers half of the fibre, confirming the high compatibility between the matrix and the fibre surface. Two long fibres are observed in the LF-tested sample in Fig. 7e. The surrounding matrix is visibly altered following the direction of the filler. A detail showing the wall of a long fibre is reported in Fig. 7f. Moreover, the high affinity between the matrix and the surface filler is recognizable. The high compatibility between the matrix and the fibrous additive is also more evident if these images are compared to the SEM investigation of the fibers alone, as illustrated in ESI Materials and Fig. S7d–f.† In Fig. 7g, the nature of the inert granules (IG) filler is evident as irregularly shaped platelets (granules alone are reported in ESI Materials, Fig. S7a–c†) emerging from the fractured surface of the broken IG 20% sample. Although the surface of platelets appears smoother compared to the fibre walls, a good affinity with the polymer is still retained, as observed in the magnification of Fig. 7h. Finally, the fractured sample containing both 20% inert granules and long fibres is observable in Fig. 7i. The pull-out of the long fibres is visible, while the granule fragments are homogeneously distributed in the matrix.

The high compatibility between the matrix and the additives (confirmed by SEM analysis) leads us to suppose that interactions are established between the protein and the additives due to many functional groups, such as abundant free amino groups, present both in the proteins and in the components of the additives (mainly lignin, cellulose, and hemicellulose).

The decrease in the glass transition temperature observed after the addition of fillers suggests that these interactions are not cross-linked; otherwise, the segmental mobility would have decreased but exhibited weak intermolecular interactions.

Proof of concept

To demonstrate the actual practical use of these materials, different prototypes of commonly used items were prepared using the most promising composite material among those analyzed, LF/IGmix (Fig. 8). Similar to what was done to obtain the specimens for the mechanical tests, the objects were prepared manually by compression moulding, starting from the material in its soft state and imparting a pressure of about 15 kPa. The material was modelled into plastic moulds to give the desired shape and air dried at room temperature. To prepare the colored objects (leaf-shaped gadgets, caps, ice cream spoons and coasters), natural food grade coloring was mixed with the material in its malleable state before the modeling phase. The prototype plates and crockery are ivory, which is the natural color of the material.

The prototypes obtained show that the material can be used for the creation of hard plastic objects, such as taps, crockery, plates, drink coasters, and playful gadgets of simple or more complex shapes. Interestingly, their storage properties have been tested in environmental temperature and under humidity conditions (RH ranging from 20 to 60%) for long periods (even three years). The objects show no deterioration or trace of mold in any way. The applications imagined for these new materials

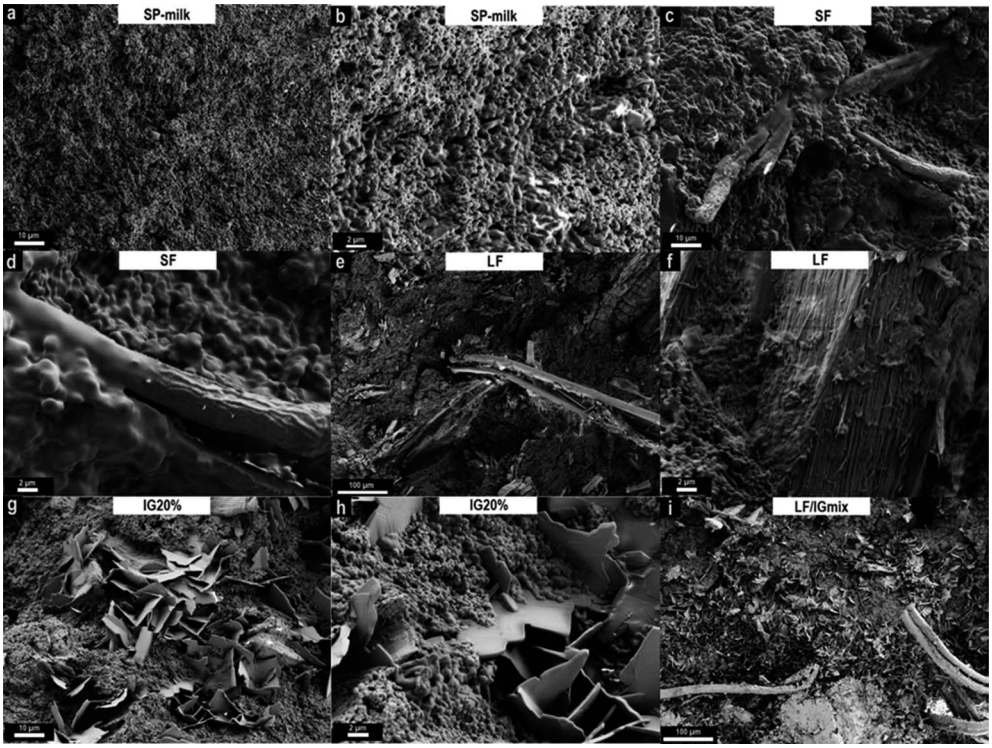

Fig. 7 FE-SEM micrographs of fractured surfaces of the samples after bending test: (a and b) SP-Milk®; (c and d) short fibre composite (SF); (e and f) long fibre composite (LF); (g and h) 20% inert granules composite (IG 20%); and (i) long fibres and 20% inert granules mixed composite (LF/IGmix).

Fig. 8 Prototypes of commonly used items obtained from the LF/IGmix composite material.

are all those in which long-lasting materials are not required, such as most of the single-use items and packaging solutions. For application in the food field, the necessary certifications are obtained (presence of potential allergens, contact with food, *etc.*). These applications are the main cause of plastic pollution[40] because they are used for an extremely short time; then, they are discarded. Moreover, these kinds of objects are often made of more than a single polymer, resulting in difficulties recycling them. In addition to these kinds of applications, we think that an interesting way to use these materials could be in the production of gadgets and toys owing to the absence of any toxic components and the mechanical resistance and thermal stability adequate for those uses.

Furthermore, the compostability of the manufactured objects shown in Fig. 8 was tested, and the objects were demonstrated to be compostable even under "home conditions", establishing that the material and the produced objects maintain this property. Recently, the material in the form of film compressed at 90 °C was tested for biodegradability at the natural seawater–sediment interface according to ISO 19679:2020. The experiment was performed by measuring the evolved CO_2 using real seawater samples. It has been demonstrated that the material can biodegrade at 83% in only 52 days under oligotrophic conditions and without the addition of other microorganisms.[41]

Conclusions

In this work, a new biobased, biodegradable, and compostable protein-based material named SP-Milk® was investigated for the first time. The SP-Milk® matrix showed mechanical properties, such as considering the material brittle. Because the use of biobased additives represents a stimulating route for creating new green composites, the effect of different natural fillers was evaluated with the aim of improving the functional properties of the SP-Milk®. It has been demonstrated that the use of suitable natural reinforcement agents is effective, leading to a general improvement in mechanical and thermal stresses. In particular, due to the strengthening properties of fibres, the addition of

natural fibrous components led to an effective reinforcement of the material given by the residual resistance effect, with an improved ductility of up to 97%. Using a combination of fibres and granules, the positive effects of both components are preserved, showing a higher elastic modulus (240 ± 20 MPa, compared to 199 ± 12 MPa for the matrix), higher ductility (+50%) and higher strain at failure (+30%). Moreover, thermal analysis proved that the selected additives enhance the thermal stability of the material and improve its workability by lowering the glass transition temperature. The main advantages of the composites made of SP-Milk® are as follows: they are fully biobased and not blended with fossil-based polymers; they are thermally stable in a temperature range useful for creating items, such as taps, crockery, plates, drink coasters and playful gadgets; and they are obtained from waste material. Compared to starch-based bioplastics, it does not involve the exploitation of farmland, avoiding the related problems of soil depletion and lowering costs in the production process. The samples analysed in this work were manually manufactured. Using industrial machines and more performing experimental conditions for their preparation (such as higher and controlled pressures), an improvement of their mechanical properties as well as a more homogeneous behaviour is expected. Finally, the extremely low cost of waste makes the material economically viable. The use of waste material to make a new type of plastic represents significant savings for manufacturing companies, which thus participate in a virtuous path that adheres to the principles of the circular economy.

Author contributions

R. Lettieri: conceptualization, methodology writing – original draft preparation. V. Fazio: investigation, formal analysis, reviewing and editing. D. Abruzzese: conceptualization, methodology, reviewing and editing. E. Di Bartolomeo: resources, reviewing and editing. C. D'Ottavi: investigation, reviewing and editing. A. Micheletti: methodology, reviewing and editing. A. Tiero: methodology, reviewing and editing. L. Duranti: investigation, formal analysis, reviewing and editing. V. Armuzza: methodology, reviewing and editing; S. Licoccia: resources, reviewing and editing. E. Gatto: conceptualization, supervision, writing – reviewing and editing. All authors have given approval to the final version of the manuscript.

Conflicts of interest

E. G. and R. L. are co-founders of the Splastica spinoff, which is the owner of the SP-Milk® patent.

Acknowledgements

This work was supported by the HORIZON EUROPE European Innovation Ecosystems "Women TechEU" SP-Milk (project no. 101072294); and "Pre-Seed" Lazio Innova POR FERS LAZIO 2014–2020 (no. A0122-2019-29272).

References

1 OECD, *Global Plastics Outlook: Economic Drivers, Environmental Impacts and Policy Options*, OECD Publishing, Paris, 2022, DOI: 10.1787/de747aef-en.
2 D. Charles and L. Kimman, *Plastic Waste Makers Index 2023*, Minderoo Foundation, 2023 [cited 2024 Apr 26]. Available from: https://www.minderoo.org/plastic-waste-makers-index.
3 European Bioplastics, in *European Bioplastics Org*, Available from: https://www.european-bioplastics.org/bioplastics/ [Accessed 2024 Feb14].
4 R. Mori, Replacing all petroleum-based chemical products with natural biomass-based chemical products: a tutorial review, *RSC Sustainability*, 2023, **1**, 179–212, DOI: 10.1039/d2su00014h.
5 A. Lamp, M. Kaltschmitt and J. Dethloff, Options to Improve the Mechanical Properties of Protein-Based Materials, *Molecules*, 2022, **27**, 446, DOI: 10.3390/molecules27020446.
6 I. Elfaleh, *et al.*, A comprehensive review of natural fibers and their composites: An eco-friendly alternative to conventional materials, *Results Eng.*, 2023, **19**, 101271, DOI: 10.1016/j.rineng.2023.101271.
7 Z. Singh and S. Bhalla, Toxicity of Synthetic Fibres & Health, *Adv. Res. Text. Eng.*, 2017, **2**(1), 1012–1015, DOI: 10.26420/advrestexteng.2017.1012.
8 F. Ortega, F. Versino, O. V. López and M. A. García, Biobased composites from agro-industrial wastes and by-products, *Emergent Mater.*, 2022, **5**, 873–921, DOI: 10.1007/s42247-021-00319.
9 F. G. Torres, S. Rodriguez and A. C. Saavedra, Green Composite Materials from Biopolymers Reinforced with Agroforestry Waste, *J. Polym. Environ.*, 2019, **27**, 2651–2673, DOI: 10.1007/s10924-019-01561-5.
10 M. Y. Khalid, A. Al Rashid, Z. U. Arif, W. Ahmed, H. Arshad and A. A. Zaidi, Natural fiber reinforced composites: Sustainable materials for emerging applications, *Results Eng.*, 2021, **11**, 100263, DOI: 10.1016/j.rineng.2021.100263.
11 A. Gholampour and T. Ozbakkaloglu, A review of natural fiber composites: properties, modification and processing techniques, characterization, applications, *J. Mater. Sci.*, 2020, **55**, 829–892, DOI: 10.1007/s10853-019-03990-y.
12 M. R. Sanjay, S. Siengchin, J. Parameswaranpillai, M. Jawaid, C. I. Pruncu and A. Khan, A comprehensive review of techniques for natural fibers as reinforcement in composites: preparation, processing and characterization, *Carbohydr. Polym.*, 2019, **207**, 108–121, DOI: 10.1016/j.carbpol.2018.11.083.
13 F. M. Al-Oqla and S. M. Sapuan, Natural fiber reinforced polymer composites in industrial applications: feasibility of date palm fibers for sustainable automotive industry, *J. Clean. Prod.*, 2014, **66**, 347–354, DOI: 10.1016/j.jclepro.2013.10.050.
14 N. Venkateshwaran, A. ElayaPerumal, A. Alavudeen and M. Thiruchitrambalam, Mechanical and water absorption behaviour of banana/sisal reinforced hybrid composites,

Mater. Des., 2011, **32**(7), 4017–4021, DOI: 10.1016/j.matdes.2011.03.002.

15 H. Bisaria, M. K. Gupta, P. Shandilya and R. K. Srivastava, Effect of Fibre Length on Mechanical Properties of Randomly Oriented Short Jute Fibre Reinforced Epoxy Composite, *Mater. Today: Proc.*, 2015, **2**(4–5), 1193–1199, DOI: 10.1016/j.matpr.2015.07.031.

16 F. Ortega, F. Versino, O. V. López and M. A. García, Biobased composites from agro-industrial wastes and by-products, *Emergent Mater.*, 2022, **5**, 873–921, DOI: 10.1007/s42247-021-00319-x.

17 K. Rafiee, H. Schritt, D. Pleissner, G. Kaur and S. K. Brar, Biodegradable green composites: It's never too late to mend, *Curr. Opin. Green Sustainable Chem.*, 2021, **30**, 100482, DOI: 10.1016/j.cogsc.2021.100482.

18 D.-M. Monika, K. Monika and B. Mateusz, Walnut shells as a filler for polymeric materials, *Drewno*, 2019, **62**(203), 153–168, DOI: 10.12841/wood.1644-3985.D12.02.

19 V. Ahlawat, S. Kajal and A. Parinam, Experimental analysis of tensile, flexural, and tribological properties of walnut shell powder/polyester composites, *Euro-Mediterr. J. Environ. Integr.*, 2018, **4**(1), 1–9, DOI: 10.1007/s41207-018-0085-6.

20 U. Koester and E. Galaktionova, FAO Food Loss Index methodology and policy implications, *Stud. Agric. Econ.*, 2021, **123**(1), 1–7, DOI: 10.7896/j.2093.

21 H. Pirayesh, H. Khanjanzadeh and A. Salari, Effect of using walnut/almond shells on the physical, mechanical properties and formaldehyde emission of particleboard, *Composites, Part B*, 2013, **45**(1), 858–863, DOI: 10.1016/j.compositesb.2012.05.008.

22 A. Valdés, O. Fenollar, A. Beltrán, R. Balart, E. Fortunati, J. M. Kenny and M. C. Garrigós, Characterization and enzymatic degradation study of poly(ε-caprolactone)-based biocomposites from almond agricultural by-products, *Polym. Degrad. Stab.*, 2016, **132**, 181–190, DOI: 10.1016/j.polymdegradstab.2016.02.023.

23 A. Valdés García, M. R. Santonja, A. B. Sanahuja and M. C. Garrigós Selva, Characterization and degradation characteristics of poly(ε-caprolactone)-based composites reinforced with almond skin residues, *Polym. Degrad. Stab.*, 2014, **108**, 269–279, DOI: 10.1016/j.polymdegradstab.2014.03.011.

24 D. Nogueira and V. G. Martins, Use of Different Proteins to Produce Biodegradable Films and Blends, *J. Polym. Environ.*, 2019, **27**, 2027–2039, DOI: 10.1007/s10924-019-01494-z.

25 A. Jerez, P. Partal, I. Martínez, C. Gallegos and A. Guerrero, Protein-based bioplastics: Effect of thermo-mechanical processing, *Rheol. Acta*, 2007, **46**, 711–720, DOI: 10.1007/s00397-007-0165-z.

26 K. Dangaran, P. M. Tomasula and P. Qi, Structure and Function of Protein-Based Edible Films and Coatings, in *Edible Films and Coatings for Food Applications*, ed. K. Huber and M. Embuscado, Springer, New York, NY, 2009, DOI: 10.1007/978-0-387-92824-1_2.

27 E. I. Goksu, M. Karamanlioglu, U. Bakir, L. Yilmaz and U. Yilmazer, Production and characterization of films from cotton stalk xylan, *J. Agric. Food Chem.*, 2007, **55**, 10685–10691, DOI: 10.1021/jf071893i.

28 X. W. Peng, J. L. Ren, L. X. Zhong and R. C. Sun, Nanocomposite Films Based on Xylan-Rich Hemicelluloses and Cellulose Nanofibers with Enhanced Mechanical Properties, *Biomacromolecules*, 2011, **12**(9), 3321–3329, DOI: 10.1021/bm2008795.

29 Y. Du, S. Li, Y. Zhang, C. Rempel and Q. Liu, Treatments of protein for biopolymer production in view of processability and physical properties: a review, *J. Appl. Polym. Sci.*, 2016, **133**, 43351, DOI: 10.1002/app.43351.

30 S. Vigneshwaran, R. Sundarakannan, K. M. John, R. Deepak Joel Johnson, K. Arun Prasath, S. Ajith, V. Arumugaprabu and M. Uthayakumar, Recent advancement in the natural fiber polymer composites: a comprehensive review, *J. Clean. Prod.*, 2020, **277**, 124109, DOI: 10.1016/j.jclepro.2020.124109.

31 E. Akdoğan, The effects of high density polyethylene addition to low density polyethylene polymer on mechanical, impact and physical properties, *Eur. J. Tech.*, 2020, **10**(1), 25–37, DOI: 10.36222/ejt.646693.

32 C. Chaléat, P. J. Halley and R. W. Truss, Chapter 7-Mechanical Properties of Starch-Based Plastics, in *Starch Polymers, from Genetic Engineering to Green Applications*, ed. P. J. Halley and L. Avérous, Elsevier, 2014, pp. 187–209, DOI: 10.1016/B978-0-444-53730-0.00023-3.

33 M. T. Kalichevsky, J. M. V. Blanshard and P. F. Tokargzuk, Effect of water content and sugars on the glass transition of casein and sodium caseinate, *Int. J. Food Sci. Technol.*, 1993, **28**(2), 139–151, DOI: 10.1111/j.1365-2621.1993.tb01259.x.

34 M. T. Kalichevsky and J. M. V. Blanshard, A study of the effect of water on the glass transition of 1:1 mixtures of amylopectin, casein and gluten using DSC and DMTA, *Carbohydr. Polym.*, 1992, **19**(4), 271–278, DOI: 10.1016/0144-8617(92)90080-A.

35 A. M. Mocanu, C. Moldoveanu, L. Odochian, C. M. Paius, N. Apostolescu and R. Neculau, Study on the thermal behavior of casein under nitrogen and air atmosphere by means of the TG-FTIR technique, *Thermochim. Acta*, 2012, **546**, 120–126, DOI: 10.1016/j.tca.2012.07.031.

36 X. Wu, Q. Liu, Y. Luo, M. S. Murad, L. Zhu and G. Mu, Improved packing performance and structure-stability of casein edible films by dielectric barrier discharges (DBD) cold plasma, *Food Packag. Shelf Life*, 2020, **24**, 100471, DOI: 10.1016/j.fpsl.2020.100471.

37 M. L. Picchio, Y. G. Linck, G. A. Monti, L. M. Gugliotta, R. J. Minari and C. I. Alvarez Igarzabal, Casein films crosslinked by tannic acid for food packaging applications, *Food Hydrocolloids*, 2018, **84**, 424–434, DOI: 10.1016/j.foodhyd.2018.06.028.

38 C. Bengoechea, A. Arrachid, A. Guerrero, S. E. Hill and J. R. Mitchell, Relationship between the glass transition

temperature and the melt flow behavior for gluten, casein and soya, *J. Cereal Sci.*, 2007, **45**, 275–284, DOI: **10.1016/j.jcs.2006.08.011**.

39 C. J. R. Verbeek and L. E. Van Den Berg, Extrusion Processing and Properties of Protein-Based Thermoplastics, *Macromol. Mater. Eng.*, 2010, **295**(1), 10–21, DOI: **10.1002/mame.200900167**.

40 Plastics Europe, Plastics – the fast facts 2023, Available from: **https://plasticseurope.org/de/knowledge-hub/plastics-the-fast-facts-2023/**.

41 A. Caravella, R. Lettieri, R. Vezza and E. Gatto, Aerobic Biodegradation at a Seawater-Sediment Interface of a New Bioplastic 100% Based on Natural Polymers, *ACS Sustainable Resour. Manage.*, 2024, DOI: **10.1021/acssusresmgt.4c00029**.